ADVANCES IN ATMOSPHERIC SCIENCES, VOL. 26, NO. 6, 2009, 1099–1107

Retrieval of Aerosol Optical Properties over the Beijing Area Using POLDER/PARASOL Satellite Polarization Measurements

FAN Xuehua*[1,2] (范学花), CHEN Hongbin[1] (陈洪滨), LIN Longfu[2] (林龙福), HAN Zhigang[1](韩志刚), and Philippe GOLOUB[3]

[1]*Key Laboratory for Middle Atmosphere and Global Environment Observation, Institute of Atmospheric Physics, Chinese Academy of Sciences, Beijing* 100029

[2]*Beijing Institute of Applied Meteorology, Beijing* 100029

[3]*Laboratoire d'Optique Atmosphérique, Université des Sciences et Technologies de Lille, UMR-CNRS* 8518*, Villeneuve d'Ascq, France*

(Received 11 July 2008; revised 9 February 2009)

ABSTRACT

Aerosol optical properties over Beijing and Xianghe under several typical weather conditions (clear sky, light haze, heavy pollution and dust storm) are derived from POLDER (POLarization and Directionality of the Earth's Reflectances)/PARASOL (Polarization and Anisotropy of Reflectances for Atmospheric Sciences coupled with Observations from a Lidar) multi-directional, multi-spectral polarized signals using a more reliable retrieval algorithm as proposed in this paper. The results are compared with those of the operational retrieval algorithm of POLDER/PARASOL group and the ground-based AERONET (AErosol RObotic NETwork)/PHOTONS (PHOtométrie pour le Traitement Opérational de Normalisation Satellitaire) measurements. It is shown that the aerosol optical parameters derived from the improved algorithm agree well with AERONET/PHOTONS measurement. The retrieval accuracies of aerosol optical thickness (AOT) and effective radius are 0.06 and 0.05 μm respectively, which are close to or better than the required accuracies (0.04 for AOT and 0.1 μm for effective radius) for estimating aerosol direct forcing.

Key words: POLDER/PARASOL, polarized reflectance, aerosol optical properties, AERONET/PHOTONS

Citation: Fan, X. H., H. B. Chen, L. F. Lin, Z. G. Han, and P. Goloub, 2009: Retrieval of aerosol optical properties over the Beijing area using POLDER/PARASOL satellite polarization measurements. *Adv. Atmos. Sci.*, **26**(6), 1099–1107, doi: 10.1007/s00376-009-8103-x.

1. Introduction

Because of high surface reflectivity and spatial variability, satellite remote sensing of aerosol properties is much more difficult over land than over ocean. The problem has been approached in several ways, for example, using thermal contrast over desert areas (Legrand et al., 1989), via the reflectance over dense dark vegetation (Kaufman et al., 1997), from data over inland lakes (Mao et al., 2001; Zhang et al., 2003), via the adjacency effect of the aerosols (Tanré et al., 1992; Holben et al., 1992), and by exploiting the small reflection of land surfaces in the UV wavelengths (Herman et al., 1997; Torres et al., 2002).

The multi-directional, multi-spectral polarized satellite sensor POLDER can acquire global observations of the polarization and directionality of solar radiation reflected by the earth-atmosphere system. The polarized light reflected by ground targets is small and stable enough to allow for correction in TOA measurements (Deuzé et al., 1993), so POLDER has provided a unique opportunity for aerosol remote sensing over land surfaces. Data collected by POLDER allows us to derive the total aerosol optical thickness and

*Corresponding author: FAN Xuehua, fxh@mail.iap.ac.cn

the Ångström exponent, an indicator of particle size, which is deduced from the spectral optical thickness (Deuzé et al., 2000; Vachon et al., 2004). Moreover, when the viewing geometry is suitable, POLDER can discriminate large spherical marine aerosols from non-spherical desert aerosols, retrieve the effective radius of the accumulation and coarse modes, and provide an estimate of the real part of the refractive index (Herman et al., 2005).

POLDER operational retrievals over land are mainly sensitive to small particles such as the aerosols created by anthropogenic pollution or biomass burning (Leroy et al., 1997; Deuzé et al., 2001; Sano, 2004). Validation against AERONET/PHOTONS observations over eastern Asia have shown that the Ångström exponent of the POLDER operational algorithm seems to be overestimated (Fan et al., 2008). In addition, discrepancies appear because of the overestimation of the surface polarization model, especially over urban areas (Holzer-Popp et al., 2008). For reduction of this deviation, an improved retrieval algorithm is developed, focusing on the Beijing region in the paper, using a surface polarization model validated over the Inner Mongolian steppe and an aerosol model considering the effective radius and effective variance. The improved algorithm is tested over sites at Beijing and Xianghe under several typical weather conditions, and some results are derived from POLDER data.

The paper is structured as follows: the POLDER instrument is briefly introduced in the second section. A description of the operational retrieval scheme applied to POLDER aerosol products is given, and the improved retrieval algorithm is presented in the third section. Retrieval results and some discussion are given in the fourth section. The work is summarized in the fifth section.

2. POLDER on-board PARASOL satellite

POLDER-1/2 on board the ADEOS-I and ADEOS-II (Advanced Earth Observation Satellite) spacecrafts are no longer acquiring data because of solar panel failure of the platform. The PARASOL satellite is a part of the so-called "A-train" series, and carries the POLDER-3 instrument consisting of a wide field-of-view telecentric optics, a rotating wheel with spectral and polarizing filters, and a 274×242 two-dimensional CCD (Charge Coupled Device) detector array (Deschamps et al., 1994). The polarization measurements are done at three wavelengths (490, 670, and 865 nm). Three elements of the Stokes parameter (I, Q, and U) are obtained. The directional measurements cover up to 51° in the along-track direction and up to 43° in the cross-track direction. The ground pixel size is about 5×6 km^2 at nadir. Multiple angle viewing is achieved by overriding successive images of the same spectral band. Thus, in a single satellite pass, any target within the instrument swath can be observed quasi-simultaneously from up to 16 viewing angles.

3. Algorithm description

3.1 *POLDER/PARASOL operational retrieval scheme*

According to the (Deuzé et al., 2001) approach developed for POLDER aerosol retrievals over land, $R_{\mathrm{P,\,TOA}}$, the polarized reflectance at top of atmosphere (TOA) can be expressed as follows:

$$R_{\mathrm{P,\,TOA}} = R_{\mathrm{P,\,surf}} T + R_{\mathrm{P,\,atmos}} \tag{1}$$

where $R_{\mathrm{P,\,surf}}$ and $R_{\mathrm{P,\,atmos}}$ are, respectively, the surface and atmospheric contributions, and T stands for the atmospheric transmittance. The surface polarized reflectance, $R_{\mathrm{P,\,surf}}$, is modeled using a semi-empirical surface model and considered to be spectrally flat. The surface polarization models for POLDER-1/2 (Bréon et al., 1995) and POLDER/PARASOL (Nadal and Bréon, 1999) are shown in formulae (2–3) and (4), respectively.

$$R_{\mathrm{p,VEG}}(\theta_{\mathrm{s}}, \theta_{\mathrm{v}}, \phi) = \frac{F_{\mathrm{p}}(\cos\gamma_0)}{4(\cos\theta_{\mathrm{s}} + \cos\theta_{\mathrm{v}})} (\mathrm{NDVI} \geqslant 0.3) \tag{2}$$

$$R_{\mathrm{p,SOIL}}(\theta_{\mathrm{s}}, \theta_{\mathrm{v}}, \phi) = \frac{F_{\mathrm{p}}(\cos\gamma_0)}{4\cos\theta_{\mathrm{s}}\cos\theta_{\mathrm{v}}} (\mathrm{NDVI} \leqslant 0.1) \tag{3}$$

$$R_{\mathrm{p}}(\theta_{\mathrm{s}}, \theta_{\mathrm{v}}, \phi) = \rho \left[1 - \exp\left(-\beta \frac{F_{\mathrm{p}}(\cos\gamma_0)}{\cos\theta_{\mathrm{s}} + \cos\theta_{\mathrm{v}}} \right) \right] \tag{4}$$

θ_{s} and θ_{v} in the above formulae are the solar zenith angle and the viewing zenith angle respectively, and ϕ is the viewing azimuth angle relative to the sun direction. $F_{\mathrm{p}}(\cos\gamma_0)$ denotes the Fresnel reflectance, as follows:

$$F_{\mathrm{p}}(\cos\gamma_0) = \frac{1}{2} \left(\left| \frac{\cos\gamma_0 - \sqrt{n^2 - 1 + \cos^2\gamma_0}}{\cos\gamma_0 + \sqrt{n^2 - 1 + \cos^2\gamma_0}} \right|^2 - \left| \frac{n^2\cos\gamma_0 - \sqrt{n^2 - 1 + \cos^2\gamma_0}}{n^2\cos\gamma_0 + \sqrt{n^2 - 1 + \cos^2\gamma_0}} \right|^2 \right), \tag{5}$$

where γ_0 is the incidence angle that is one half of the phase angle; and n is the complex refractive index of the medium whose imaginary part is zero and whose real part is dependent on the wavelength (λ) as in formula (6) (Vanderbilt and Grant, 1985):

$$n(\lambda) = 1.4576 + 0.0209\lambda^{-1.48}\,. \tag{6}$$

When NDVI (Normalized Difference Vegetation Index) is larger than 0.3, the vegetation surface model $[R_{\mathrm{p,VEG}}(\theta_{\mathrm{s}}, \theta_{\mathrm{v}}, \phi)]$ in formula (2) is used as an estimate of the surface polarized reflectance; when NDVI is lower than 0.1, the bare soil model $[R_{\mathrm{p,SOIL}}(\theta_{\mathrm{s}}, \theta_{\mathrm{v}}, \phi)]$ in formula (3) is used. For intermediate values, a linear combination is applied. In formula (4), ρ and β are empirical constants.

For POLDER/PARASOL operational data processing, the pure atmospheric contribution ($R_{\mathrm{P,\ atmos}}$) is computed with a radiative transfer code for a given geometry (θ_{s}, θ_{v}, ϕ), at 670 and 865 nm (Deuzé et al., 1989), a set of 10 aerosol models assuming spherical particles, and a set of increasing AOT (τ_{a}). Each aerosol model is described by a monomodal lognormal size distribution (with geometric standard deviation σ=0.40) and various modal radii ranging from 0.05 to 0.15 μm (associated Ångström exponent α ranging from 3.0 to 1.8). The refractive index (m) is 1.47-0.01i corresponding to small particle absorption.

Polarized reflectances are computed for increasing values of τ_a and for each aerosol model. The best agreement (i.e., minimum difference) between computed and measured spectral polarized reflectances provides AOT and Ångström exponent estimates.

3.2 *The improved retrieval algorithm*

For illustrating the sensitivity of the scattering phase matrix to the aerosol size distribution, the four size distributions Hansen and Travis, 1974; Duan, 2001 with the same effective radius (r_{eff}=0.125 μm) and effective variance (ν_{eff}=0.25) are considered. As shown in the Fig. 1, these are the Hansen-Gamma distribution, Junge distribution, monomodal lognormal distribution and bimodal lognormal distribution, respectively.

The phase function (the left panel of Fig. 2) and polarized phase function (the right panel of Fig. 2, also

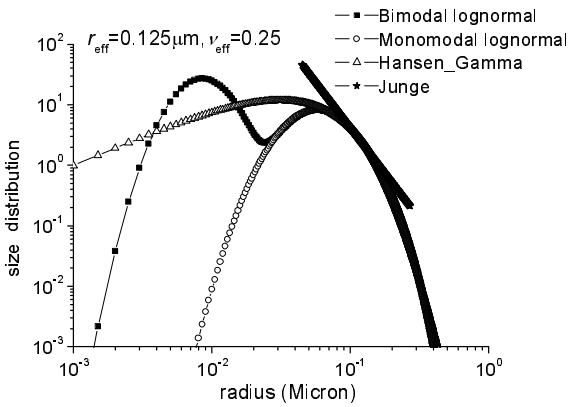

Fig. 1. The four kinds of aerosol size distribution with the same effective radius and effective variance.

called the F_{12} element of the scattering matrix) of the four size distributions for three polarized channels of the POLDER instrument are computed using the Mie code. The phase functions of the different size distributions are very close at the three wavelengths, and so are the polarized phase functions. The computational results in Fig. 2 show that the different size distributions with the same r_{eff} and ν_{eff} yield similar scattering characteristics. This conclusion is consistent with that presented by Hansen and Travis (1974). Thus, the size distribution dependent on effective radius and effective variance is used in the improved algorithm.

The Hansen-Gamma size distribution shown in formula (7) is used in the forward model:

$$n(r) = Cr^{\alpha} \exp\left(-\beta r^{\gamma}\right) \tag{7}$$

In formula (7),

$$C = \frac{\gamma \beta^{(\alpha+1)/\gamma}}{\Gamma\left(\frac{\alpha+1}{\gamma}\right)}\,, \quad \gamma = 1\,,$$
$$\alpha = \frac{1-3\nu_{\mathrm{eff}}}{\nu_{\mathrm{eff}}}\,, \quad \beta = \frac{1}{r_{\mathrm{eff}}\nu_{\mathrm{eff}}}\,,$$

where r_{eff} and ν_{eff} are the effective radius and the effective variance respectively.

The atmospheric contribution ($R_{\mathrm{P,\ atmos}}$) is computed with a vector radiative transfer model called RT3 developed by Evans and Stephens (1991) and improved by Han (1999) and Fan (2006). The improved RT3 model decomposes the atmosphere into eight layers. For aerosols, the scale height is 2 km. Aerosol optical thickness follows an exponential decay from 0 to 2 km. Above the aerosol scale height, the optical thickness at every layer is provided by the standard atmosphere. The surface polarized reflectance, $R_{\mathrm{P,\ surf}}$, is modeled using a surface model presented by Han (1999) in formula (8) and validated by the polarization measurements over the Inner Mongolian steppe.

$$R_{\mathrm{p}}(\theta_{\mathrm{s}}, \theta_{\mathrm{v}}, \phi) = \frac{K}{4(\cos\theta_{\mathrm{s}} + \cos\theta_{\mathrm{v}})} \times \left\{1 - \exp\left[-\frac{\mathrm{LAI}(\cos\theta_{\mathrm{s}} + \cos\theta_{\mathrm{v}})}{2\cos\theta_{\mathrm{s}}\cos\theta_{\mathrm{v}}}\right]\right\} \times F_{\mathrm{p}}(\cos\gamma_0)\,. \tag{8}$$

In (8), K is the corrected coefficient of leaf surface, assumed as a constant ranging from 0 to 1, and the leaf area index (LAI) is assumed to be a constant with a value of 3.2.

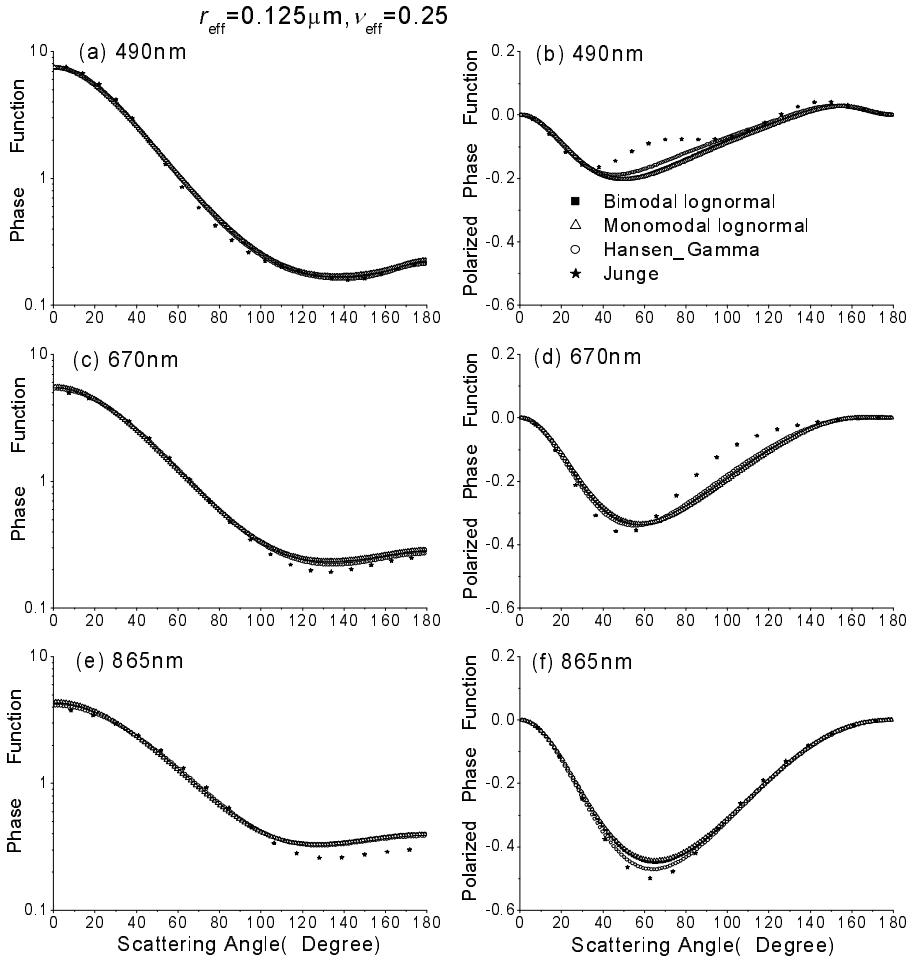

Fig. 2. Phase function (left panels) and polarized phase function (right panels) of different size distributions with the same effective radius ($r_{\rm eff}$=0.125 μm) and effective variance ($\nu_{\rm eff}$=0.25) for three polarized channels of the POLDER instrument.

4. Retrieval results and discussion

4.1 *POLDER/PARASOL level 1 polarization data*

The data used in this study are POLDER/PARASOL Level 1 products, including calibration, radiometric, and geometric processing. The normalized polarized reflectance is defined by the second and third Stokes parameters (Q and U), as follows:

$$R_{\rm p} = \frac{\pi\sqrt{Q^2+U^2}}{E_{\rm s}\cos\theta_{\rm s}}\ , \tag{9}$$

where $E_{\rm s}$ is the solar irradiance at TOA. Similarly, the first Stokes parameter, I, is converted into total reflectance:

$$R = \frac{\pi I}{E_s\cos\theta_s}\ . \tag{10}$$

The satellite viewing geometry and some auxiliary data are also given by the Level 1 data. The scattering angle Θ is computed for the viewing and solar geometry by

$$\cos\Theta = \cos\theta_{\rm s}\cos\theta_{\rm v} + \sin\theta_{\rm s}\sin\theta_{\rm v}\cos(\phi_{\rm s}-\phi_{\rm v})\ , \tag{11}$$

where $\phi_{\rm s}$ and $\phi_{\rm v}$ are, respectively, the solar and viewing azimuth angles.

4.2 *Construction of Look-Up Table* (*LUT*)

The effective variance of the Hansen-Gamma size distribution is fixed to 0.20, and the aerosol complex refractive index is $(1.50-0.01i)$. The effective radius ranges from 0.01 to 1.00 μm with steps of 0.01 μm. The AOTs at 670 and 865 nm range from 0.01 to 1.00 and 0.01 to 0.80 with steps of 0.01. According to the viewing geometry of POLDER ($\theta_{\rm s}$, $\theta_{\rm v}$, ϕ), the polarized reflectances $\{R_{\rm P\_cal}[\tau_\lambda, r_{\rm eff}(\lambda), \Theta_i]\}$ at different viewing angles are calculated to form a LUT, where the subscript "P_cal" denotes the calculated polarized reflectances.

4.3 *Aerosol optical properties retrieval*

The cloud-free POLDER pixels selected according to the cloud-screening algorithm of Bréon and Colzy (1999) are considered, and a preliminary correction of the influence of gaseous absorption (Leroy et al., 1997) is performed. To reduce the noise level, the aerosol algorithm is applied to 3×3 POLDER cloud-free pixels. The pixel-averaged polarized reflectance at 670 and 865 nm is denoted by $R_{\mathrm{P\_mea}}(\lambda, \Theta_i)$, where the subscript "P_mea" denotes the measured polarized reflectances by POLDER/PARASOL; and here the subscript i ranges from 1 to N_{dir}, which is the number of the available viewing angles.

In order to find the unknowns $r_{\mathrm{eff}}(\lambda)$ and τ_λ, the following criterion is used:

$$\sqrt{\frac{1}{N_{\mathrm{dir}}}\sum_{i=1}^{N_{\mathrm{dir}}}[R_{\mathrm{P\_cal}}(\tau_\lambda, r_{\mathrm{eff}}(\lambda), \Theta_i) - R_{\mathrm{P\_mea}}(\lambda, \Theta_i)]^2} \leqslant \varepsilon \,. \tag{12}$$

All the cases of $r^k_{\mathrm{eff}}(\lambda)$ and τ^k_λ with superscript k the solution number conforming to the discriminant (12) are found based on the minimum difference between the LUT $\{R_{\mathrm{P\_cal}}[\tau_\lambda, r_{\mathrm{eff}}(\lambda), \Theta_i]\}$ and satellite measurements $[R_{\mathrm{P\_mea}}(\lambda, \Theta_i)]$. The averaged values $\overline{r^k_{\mathrm{eff}}(\lambda)}$ and $\overline{\tau^k_\lambda}$ in formulae (13) and (14) for all the solutions are the retrieved effective radius and AOT, respectively. The standard deviations of the two parameters $\{\sigma[r^k_{\mathrm{eff}}(\lambda)]$ and $\sigma(\tau^k_\lambda)\}$ provide the uncertainties of retrieval results. The Ångström exponent can be derived from the AOT at 670 and 865 nm.

$$r_{\mathrm{eff}}(\lambda) = \overline{r_{\mathrm{eff}}(\lambda)} \pm \sigma[r^k_{\mathrm{eff}}(\lambda)] \tag{13}$$

$$\tau_\lambda = \overline{\tau^k_\lambda} \pm \sigma(\tau^k_\lambda) \tag{14}$$

The clear sky (3 Septmber 2005 and 8 October 2005), light haze (3 March 2006 and 20 April 2006), dust storm (17 May 2006), and heavy pollution (4 November 2005) days over Beijing (39.98°N, 116.38°E) and Xianghe (39.75°N, 116.96°E) are selected to test the improved retrieval algorithm. The satellite viewing geometry over Beijing and Xianghe for these days is shown in Figs. 3a and 3b, respectively. The averaged solar zenith angles of satellite measurements are 33.45°, 49.30°, 57.35°, 47.88°, 31.08°, and 22.44°, respectively, in Beijing for the 6 days. The values are 33.33°, 49.32°, 57.26°, 47.74°, 31.05°, and 22.41°, respectively, in Xianghe. The number of available viewing directions ranges from 14 to 15 for these cases.

The derived AOT (Fig. 4a) and effective radius (Fig. 4b) using the improved algorithm from 6-day POLDER/PARASOL measurements of overpasses at Beijing and Xianghe are compared with those of AERONET/PHOTONS and the POLDER/PARASOL group retrievals. It is notable that the POLDER/PARASOL group provided the AOT only at 865 nm. The consistency between the

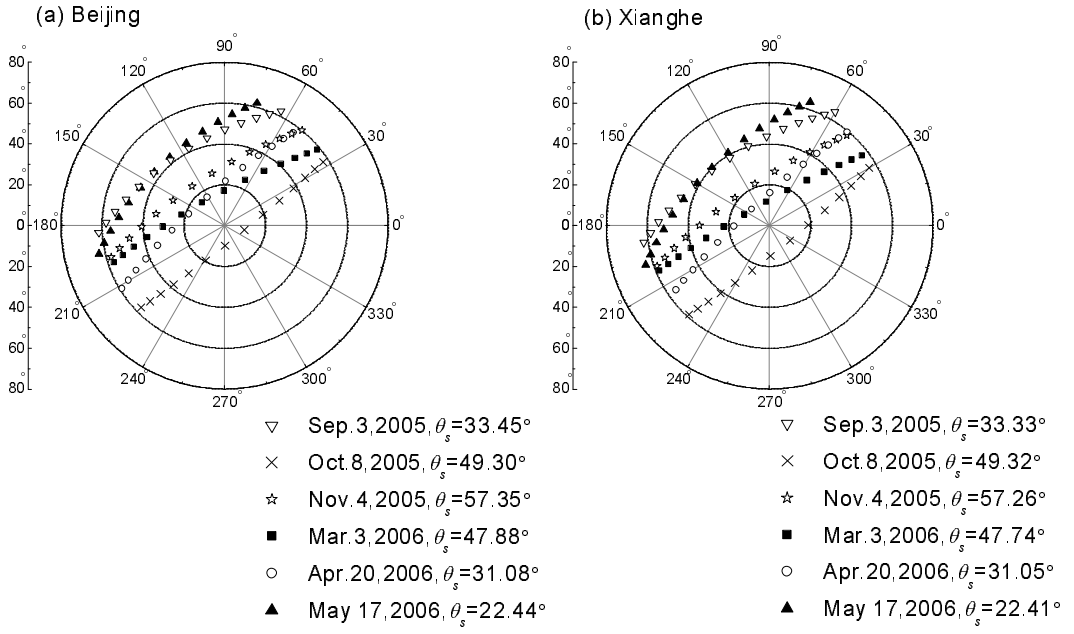

Fig. 3. Polar diagram of the POLDER/PARASOL viewing geometry in (a) Beijing and (b) Xianghe for the days used in the retrievals, where the radius of the plot is the viewing zenith angle ranging from 0° to 80° and the polar angle of the plot is the viewing azimuth angle relative to the sun direction ranging from 0° to 360°.

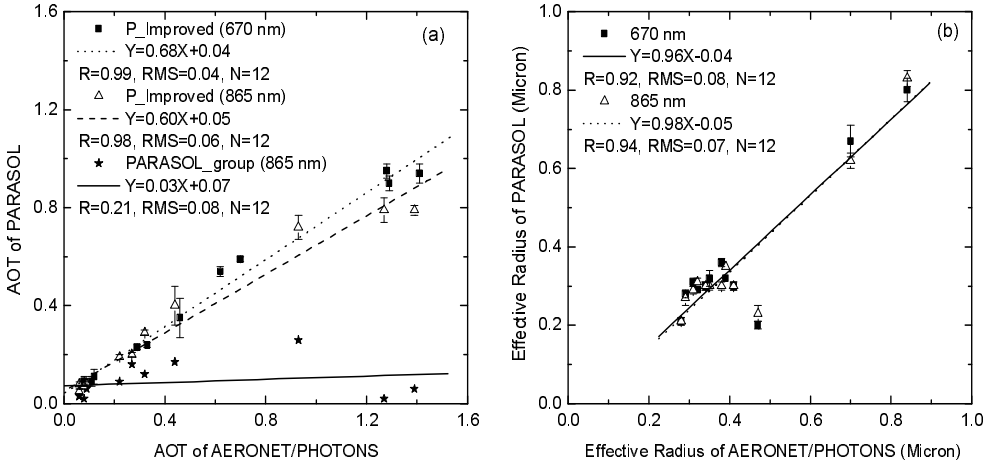

Fig. 4. (a) The AOT and (b) effective radius retrieved by the improved method are compared with those of AERONET/PHOTONS and the POLDER/PARASOL group.

Table 1. Comparison of Ångström exponents from POLDER/PARASOL retrievals using the operational algorithm and the improved method (P_Improved), as well as with AERONET/PHOTONS measurements in Beijing.

	Date						
	3 Sep 2005 (Clear)	8 Oct 2005 (Clear)	4 Nov 2005 (Pollution)	3 Mar 2006 (Haze)	20 Apr 2006 (Haze)	17 May 2006 (Dust)	Standard Deviation
AERONET/ PHOTONS	1.13	1.13	1.24	1.34	0.79	0.06	–
POLDER/ PARASOL	1.81	1.81	1.81	2.30	1.81	1.81	1.12
P_Improved	1.25	2.3	0.42	1.18	0.71	0.51	0.68

POLDER/PARASOL operational retrieval and the AERONET/PHOTONS results is very poor, since the correlation coefficient and slope are only 0.21 and 0.03. The AOTs at the two wavelengths retrieved by the improved method (P_Improved) are closer to those of the AERONET/PHOTONS ground-based measurements. The correlation coefficients are close to 1 and the slopes increase to about 0.60. It can be seen from Fig. 4b that there is general good agreement on effective radius between the improved method and AERONET/PHOTONS. In addition, the retrieved effective radii at 670 and 865 nm on the same day are very close, which is consistent with the definition that effective radius is independent of wavelength.

The comparisons of Ångström exponents for Beijing and Xianghe are shown in Tables 1 and 2. If the AERONET/PHOTONS measurements are regarded as true values, the standard deviations of the Ångström exponents retrieved by the POLDER/PARASOL operational scheme and the improved method are, respectively, 1.12 and 0.68 for Beijing. Equivalent results are found at Xi-

Table 2. Comparison of Ångström exponents from POLDER/PARASOL retrievals using the operational algorithm and improved method (P_Improved), as well as with AERONET/PHOTONS measurements in Xianghe.

	Date						
	3 Sep 2005 (Clear)	8 Oct 2005 (Clear)	4 Nov 2005 (Pollution)	3 Mar 2006 (Haze)	20 Apr 2006 (Haze)	17 May 2006 (Dust)	Standard Deviation
AERONET/ PHOTONS	1.13	1.25	1.00	1.42	1.08	0.06	–
POLDER/ PARASOL	1.81	2.30	1.81	2.42	2.30	1.81	1.25
P_Improved	0.46	0.99	1.08	0.74	0.75	0.68	0.54

anghe, where the standard deviations are, respectively, 1.25 and 0.54. It can be seen that the derived Ångström exponents are also improved generally. However, the Ångström exponents derived from the improved method are very different from those of AERONET/PHOTONS on 8 October 2005 and 4 Novembor 2005 over Beijing, and on 3 September 2005 over Xianghe. For the clear days with low AOT (8 October 2005 over Beijing and 3 September 2005 over Xianghe), the large discrepancies may have resulted from the effect of the surface polarization contribution, since the surface contribution is relatively more important in this condition. Minor errors in surface polarization can lead to high errors in the Ångström exponent. For the days with high AOT (4 November 2005, 3 March 2006), the high uncertainty of the retrieved AOT results in errors in the Ångström exponent. The accuracy of the retrieved Ångström exponent from satellite is still poor, and hence improvement of size retrieval is an urgent subject for POLDER/PARASOL (Sano, 2004).

4.4 *Discussion*

Compared with the POLDER/PARASOL operational aerosol products, the AOT and Ångström exponent results retrieved by the improved method are closer to those from AERONET/PHOTONS. The retrieved effective radii at 670 and 865 nm are very close on the same days, which is consistent with the definition that effective radius is independent of wavelength.

If the dust storm day is excluded, the retrieval accuracies of AOT and effective radius are 0.06 and 0.05 μm respectively, which are close to or better than the required accuracies (0.04 for AOT, 0.1 μm for effective radius, Mishchenko et al., 2005) for estimating aerosol direct forcing.

The improvement on aerosol properties retrieval can be explained by the following two reasons. First, the Ångström exponents ranging from 1.8 to 3.0 in the aerosol model of the POLDER/PARASOL operational algorithm are overestimated over Beijing because the statistically averaged Ångström exponent for 4-year AERONET/PHOTONS data over Beijing is about 1.2 (Fan et al., 2006). The overestimation of the Ångström exponents results in the limitation that fine-mode aerosols are dominant and AOT is underestimated. Second, the surface polarized model used in the improved scheme is different from that of the POLDER/PARASOL group. The different surface polarized models have been given in sections 3.1 and 3.2.

Take the clear day (8 October 2005) over Beijing for example, the different surface polarized models are shown in Fig. 5. The surface polarized model used in the improved scheme was validated by the measurements using the CAS/IAP photo-polarimeter during the IMGRASS'1998 (Inner-Mongolia GRassland Atmosphere Surface Study) campaign (Han, 1999). The surface polarized contribution of the models for the POLDER/PARASOL operational scheme is higher than that of the model using the improved algorithm. Waquet et al. (2007) demonstrated that the surface polarization of the POLDER operational scheme is overestimated by a few to fifty percent according to the aircraft polarized observations in France. The overestimation of surface polarization leads to AOT underestimation in the POLDER/PARASOL operational retrieval.

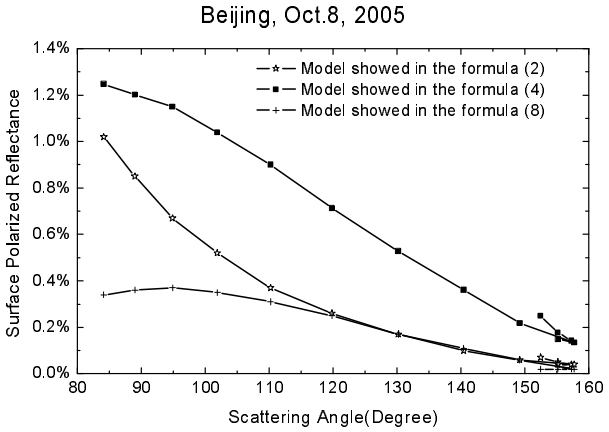

Fig. 5. Comparison of surface polarized reflectances from different surface polarization models over Beijing on a clear day (8 October 2005).

5. Summary

The aerosol optical properties over the Beijing and Xianghe sites under several typical weather conditions (clear sky, light haze, heavy pollution and dust storm) are derived from the POLDER/PARASOL multi-directional, multi-spectral polarized signals. The forward model system is improved in the aerosol model and surface polarization model. The improved aerosol model based on effective radius and effective variance is reasonable since it takes account of the contribution from coarse-mode particles to some extent. The surface polarization model employed improved the retrieval, too. The retrieved AOT at 670 and 865 nm, and the Ångström exponents over the Beijing and Xianghe sites are much closer to those of AERONET/PHOTONS than the POLDER/PARASOL operational retrieval.

Acknowledgements. This work was mainly supported by National Natural Science Foundation of China (Grant No. 40805010) and the 973 Program of China under

Grant No. 2006CB403702. The AERONET/PHOTONS team is acknowledged for the high quality sun-photometer dataset. We would like to thank the ICARE center for providing the POLDER/PARASOL level 1 data used in this study. We are grateful to the anonymous reviewers for their constructive comments and Ms. YU Ke for her help in modifying the English.

REFERENCES

Bréon, F. M., and S. Colzy, 1999: Cloud detection from the spaceborne POLDER instrument and validation against surface synoptic observations. *J. Appl. Meteor.*, **38**, 777–785.

Bréon, F. M., D. Tanré, P. Lecomte, and M. Herman, 1995: Polarized reflectance of bare soils and vegetation: measurements and models. *IEEE Trans. Geosci. Remote Sens.*, **33(2)**, 487–499.

Deschamps, P. Y., F. M. Bréon, M. Leroy, A. Podaire, A. Bricaud, J. C. Buriez, and G. Sèze, 1994: The POLDER mission: Instrument characteristics and scientific objectives. *IEEE Trans. Geosci. Remote Sens.*, **32**, 598–615.

Deuzé, J. L., M. Herman, and R. Santer, 1989: Fourier series expansion of the transfer equation in the atmosphere-ocean system. *Joural of Quantitative Spectroscopy and Radiative Transfer*, **41**, 483–494.

Deuzé, J. L., F. M. Bréon, P. Y. Deschamps, C. Devaux, M. Herman, A. Podaire, and J. L. Roujean, 1993: Analysis of the POLDER (POLarization and directionality of earth's reflectances) airborne instrument observations over land surfaces. *Remote Sens. Environ.*, **45**(2), 137–154.

Deuzé, J. L., P. Goloub, M. Herman, A. Marchand, G. Perry, S. Susana, and D. Tanré, 2000: Estimate of the aerosol properties over the ocean with POLDER. *J. Geophys. Res.*, **105**(D12), 15329–15346.

Deuzé, J. L., and Coauthors, 2001: Remote sensing of aerosols over land surfaces from POLDER/ADEOS-1 polarized measurements. *J. Geophys. Res.*, **106**(D5), 4913–4926.

Duan, M. Z., 2001: Simultaneously retrieval of atmospheric aerosols optical thickness and surface albedo over land by using polarized radiance as well as scalar radiance from satellite measurements. Ph. D dissertation, Institute of Atmospheric Physics, Chinese Academy of Sciences, 108pp. (in Chinese)

Evans, K. F., and G. L. Stephens, 1991: A new polarized atmospheric radiative transfer model. *Journal of Quantitative Spectroscopy and Radiative Transfer*, **46**(5), 413–423.

Fan, X. H., 2006: Retrieval of aerosol optical properties over Beijing from polarized signals of PARASOL. Ph. D dissertation, Institute of Atmospheric Physics, Chinese Academy of Sciences, 103pp. (in Chinese)

Fan, X. H., H. B. Chen, P. Goloub, X. A. Xia, W. X. Zhang, and B. Chatenet, 2006: Analysis of column-integrated aerosol optical thickness in Beijing from AERONET observations. *China Particuology*, **4**(6), 330–335.

Fan, X. H., P. Goloub, J. L. Deuzé, H. B. Chen, D. Tanré, and Z. Q. Li, 2008: Evaluation of PARASOL aerosol retrieval over North East Asia. *Remote Sens. Environ.*, **112**, 697–707.

Han, Z. G., 1999: Aerosol retrievals over steppe with POLDER data—Simulation model system and preliminary tests. Ph. D dissertation, Institute of Atmospheric Physics, Chinese Academy of Sciences, 104pp. (in Chinese)

Hansen, J. E., and L. D. Travis, 1974: Light scattering in planetary atmospheres. *Space Sci. Rev.*, **16**, 527–610.

Herman, J. R., P. K. Bhartia, O. Torres, C. Hsu, C. Seftor, and E. Celarier, 1997: Global distribution of UV-absorbing aerosols from Nimbus 7/TOMS data. *J. Geophys. Res.*, **102**(D14), 16911–16922.

Herman, M., J. L. Deuzé, A. Marchand, B. Roger, and P. Lallart, 2005: Aerosol remote sensing from POLDER/ADEOS over the ocean: Improved retrieval using a nonspherical particle model. *J. Geophys. Res.*, **110**(D10S02), doi: 10.1029/2004JD004798.

Holben, B. N., E. Vermote, Y. J. Kaufman, D. Tanré, and V. Kalb, 1992: Aerosol retrieval over land from AVHRR data-application for atmospheric correction. *IEEE Trans. Geosci. Remote Sens.*, **30**, 212–222.

Holzer-Popp, T., M. Schroedter-Homscheidt, H. Breitkreuz, D. Martynenko, and L. Klüser, 2008: Synergetic aerosol retrieval from SCIAMACHY and AATSR onboard ENVISAT. *Atmospheric Chemistry and Physics Discussions*, **8**, 2903–2951.

Kaufman, Y. J., D. Tanré, L. A. Remer, E. F. Vermote, A. Chu, and B. N. Holben, 1997: Operational remote sensing of tropospheric aerosol over land from EOS Moderate Resolution Imaging Spectroradiometer. *J. Geophys. Res.*, **102**, 17051–17067.

Legrand, M., J. J. Bertrand, M. Desbois, L. Menenger, and Y. Fouquart, 1989: The Potential of infrared satellite data for the retrieval of Saharan-dust optical depth over Africa. *J. Appl. Meteor.*, **28**, 309–318.

Leroy, M., and Coauthors, 1997: Retrieval of atmospheric properties and surface bi-directional reflectances over land from POLDER/ADEOS. *J. Geophys. Res.*, **102**(D14), 17023–17037.

Mao, J. T., L. Liu, and J. H. Zhang, 2001: GMS5 remote sensing of aerosol optical thickness over ChaoHu lake. *Acta Meteorologica Sinica*, **59**(3), 352–359. (in Chinese)

Mishchenko, M. I., B. Cairns, J. Chowdhary, I. V. Geogdzhayev, L. Liu, and L. D. Travis, 2005: Remote sensing of terrestrial tropospheric aerosols from aircraft and satellites. *Journal of Physics: Conference Series*, **6**, 73–89.

Nadal, F., and F. M. Bréon, 1999: Parameterization of surface polarized reflectances derived from POLDER spaceborne measurements. *IEEE Trans. Geosci. Remote Sens.*, **37**, 1709–1719.

Sano, I., 2004: Optical thickness and Ångström exponent

of aerosols over the land and ocean from space-borne polarimetric data. *Adv. Space Res.*, **34**, 833–837.

Tanré, D., E. Vermote, and B. N. Holben, 1992: Satellite aerosol retrieval over land surfaces using the structure functions. *Proc. IGARSS'92, IEEE Trans. Geoscience Remote Sensing Society*, Houston, TX, 1474–1477.

Torres, O., P. K. Bhartia, J. R. Herman, A. Sinyuk, P. Ginoux, and B. N. Holben, 2002: A long-term record of aerosol optical depth from TOMS observations and comparison to AERONET Measurements. *J. Atmos. Sci.*, **59**, 398–413.

Vachon, F., A. Royer, M. Aubé, B. Toubbé, N. T. O'Neill, and P. M. Teillet, 2004: Remote sensing of aerosols over North American land surfaces from POLDER and MODIS measurements. *Atmos. Environ.*, **38**, 3501–3515.

Vanderbilt, V. C., and L. Grant, 1985: Plant canopy specular reflectance model. *IEEE Trans. Geosci. Remote Sens.*, **GE23**(5), 722–730.

Waquet, F., P. Goloub, J. L. Deuzé, J. F. Léon, F. Auriol, C. Verwaerde, J. Y. Balois, and P. François, 2007: Aerosol Retrieval Over Land using a multiband polarimeter and comparison with path radiance method. *J. Geophys. Res.*, **112**, doi: 10.1029/2006JD008029.

Zhang, J. H., Z. J. Si, J. T. Mao, and M. H.Wang, 2003: Remote sensing aerosol optical depth over China with GMS-5 satellite. *Chinese J. Atmos. Sci.*, **27**(1), 23–35. (in Chinese)